On merger bias and the clustering of quasars

Silvia Bonoli[1]*, Francesco Shankar[1], Simon D.M. White[1], Volker Springel[1],
J. Stuart B. Wyithe[2]

[1]*Max-Planck-Institut für Astrophysik, Karl-Schwarzschild Strasse 1, D-85740 Garching, Germany*
[2]*School of Physics, University of Melbourne, Parkville, Victoria, Australia*

31 August 2009

ABSTRACT
We use the large catalogues of haloes available for the Millennium Simulation to test whether recently merged haloes exhibit stronger large-scale clustering than other haloes of the same mass. This effect could help to understand the very strong clustering of quasars at high redshift. However, we find no statistically significant excess bias for recently merged haloes over the redshift range $2 \leqslant z \leqslant 5$, with the most massive haloes showing an excess of at most $\sim 5\%$. We also consider galaxies extracted from a semianalytic model built on the Millennium Simulation. At fixed stellar mass, we find an excess bias of $\sim 20-30\%$ for recently merged objects, decreasing with increasing stellar mass. The fact that recently-merged galaxies are found in systematically more massive haloes than other galaxies of the same stellar mass accounts for about half of this signal, and perhaps more for high-mass galaxies. The weak merger bias of massive systems suggests that objects of merger-driven nature, such as quasars, do not cluster significantly differently than other objects of the same characteristic mass. We discuss the implications of these results for the interpretation of clustering data with respect to quasar duty cycles, visibility times, and evolution in the black hole-host mass relation.

Key words: cosmology: theory - cosmology: dark matter - galaxies: formation - galaxies: high-redshift - quasars: general

1 INTRODUCTION

In the last decade, much theoretical work has tried to constrain the cosmological evolution of supermassive black holes (BHs) by simultaneously interpreting the statistics of quasars/BHs and their clustering as a function of redshift and luminosity (e.g., Kauffmann & Haehnelt 2002a; Wyithe & Loeb 2005; Lidz et al. 2006; Hopkins et al. 2007; Thacker et al. 2009; Bonoli et al. 2009; Shankar et al. 2008, 2009). In fact, if quasars are hosted by haloes whose bias is only mass-dependent, clustering measurements can be used to infer the mass $M_{\rm Halo}$ of the host dark matter halo, which in turn provides host number densities, quasar duty cycles (here defined as the ratio between quasar and halo number densities) and scatter in the relation between quasar luminosity L and halo mass (Cole & Kaiser 1989; Haehnelt et al. 1998; Martini & Weinberg 2001; Haiman & Hui 2001). Measuring a high bias implies high halo masses, low host number densities, high duty cycles, and vice versa. At fixed duty cycle, increasing the scatter in the mean L-$M_{\rm Halo}$ relation implies increasing the contribution of less massive and less biased haloes to the same luminosity bin, thus lowering the overall bias.

The advent of wide-field surveys like the Sloan Digital Sky Survey (SDSS) and the 2dF quasi-stellar object (2dFQSO) (York et al. 2000; Croom et al. 2004) survey, with the detection of

thousands of quasars, has allowed a detailed investigation of the clustering properties of accreting BHs from the local universe up to $z \sim 5$ (e.g., Porciani et al. 2004; Croom et al. 2005; Shen et al. 2007; Myers et al. 2007; Coil et al. 2007; da Ângela et al. 2008; Padmanabhan et al. 2008; Ross et al. 2009). Assuming that haloes hosting quasars are typical in the way they trace the dark matter density field, these studies concluded that quasars reside at all times in a relatively narrow range of halo masses, $M_{\rm Halo} \sim 3 \times 10^{12} - 10^{13} h^{-1} {\rm M_\odot}$.

Interestingly, the very high clustering amplitude of luminous quasars at $z > 3$ measured with the SDSS (Shen et al. 2007) has posed some nagging theoretical problems for the simultaneous interpretation of the clustering and the luminosity function at these epochs. The high clustering appears to imply that the quasars live in very massive haloes. But the extreme rareness of such haloes is difficult to reconcile with the observed quasar luminosity function, especially at $z \sim 4$, unless a high quasar duty cycle and a very low scatter in the L-$M_{\rm Halo}$ relation are assumed (White et al. 2008). Moreover, matching the high $z \gtrsim 3-4$ quasar emissivity to the low number density of hosts constrains the ratio of the radiative efficiency of accretion ε to the Eddington ratio λ to be $\varepsilon > 0.7\lambda/(1+0.7\lambda)$, implying $\varepsilon > 0.17$ for $\lambda > 0.25$ (Shankar et al. 2008), which are rather extreme values. However, these conclusions can be relaxed if quasar hosts cluster more strongly than typical haloes of similar mass (Wyithe & Loeb 2009). This would then

imply that quasars live in less massive but more numerous haloes, allowing for lower duty cycles and less extreme values for ε.

Several analytical and numerical studies have investigated whether haloes of similar mass have different large-scale clustering properties, depending, in a non-trivial way, on their growth history, concentration, spin, or environment (e.g., Kolatt et al. 1999; Lemson & Kauffmann 1999; Kauffmann & Haehnelt 2002b; Gao et al. 2005; Wechsler et al. 2006; Gao & White 2007; Angulo et al. 2008). In particular, Wyithe & Loeb (2009) suggest that the possible merger-driven nature of quasars might cause an excess bias, if the large-scale clustering of recently-merged haloes is higher than expected for typical haloes of the same mass ("merger bias"). This suggestion was based on the model by Furlanetto & Kamionkowski (2006), who analytically calculated that close merging pairs might possess a merger bias of a factor of $\gtrsim 1.5$.

Recent work has indeed shown that clustering strength depends not only on halo mass, but also on other parameters. Gao et al. (2005) found that later forming haloes with mass $M < M*$ are less clustered than typical haloes of the same mass ("assembly bias"). Wechsler et al. (2006) extended this study to show that less concentrated haloes more massive than the non-linear mass scale are instead more biased than average. Li et al. (2008) explored various definitions of halo formation time, and concluded that the dependence of clustering on halo history depends strongly on the precise aspect of the history that is probed: while they confirmed previous results on assembly bias, they did not find any dependence of clustering on the time of the last major merger. Other numerical work that specifically looked at merger bias found inconclusive results, probably due to the different ranges of masses, redshifts and scales used and the poor statistics available (Gottlöber et al. 2002; Percival et al. 2003; Scannapieco & Thacker 2003). Wetzel et al. (2007) used a large dark matter simulation to study the clustering of very massive haloes ($M_{\rm Halo} > 5.0 \times 10^{13} h^{-1} {\rm M}_\odot$), and found that, at redshift $z \lesssim 1$, merger remnants show an excess bias of $\sim 5-10\%$.

In this work we make use of the large, publicly available catalogues of the Millennium Simulation (Springel et al. 2005) to explore for a wider range of masses the level of excess bias for high redshift merger remnants. In Section 2 we briefly describe the simulation and how we identify recent mergers both of haloes and galaxies. In Section 3 we show results for the merger bias both of haloes and of galaxies, and in Section 4 we discuss the implications of our results for the clustering of quasars. A summary and our conclusions are presented in Section 5.

2   IDENTIFYING MERGING HALOES AND GALAXIES IN THE MILLENNIUM SIMULATION

2.1   The Millennium Simulation and its galaxy population

The Millennium Simulation (Springel et al. 2005) is an N-body simulation which follows the cosmological evolution of $2160^3 \simeq 10^{10}$ dark matter particles, each with mass $\sim 8.6 \times 10^8 h^{-1} {\rm M}_\odot$, in a periodic box of $500 h^{-1}$Mpc on a side. The cosmological parameters used in the simulation are consistent with the WMAP1 & 2dF-GRS 'concordance' ΛCDM framework: $\Omega_m = 0.25$, $\Omega_\Lambda = 0.75$, $\sigma_8 = 0.9$, Hubble parameter $h = H_0/100 \,{\rm km s}^{-1}{\rm Mpc}^{-1} = 0.73$ and primordial spectral index $n = 1$ (Spergel et al. 2003). In the present work we focus on the clustering of galaxies and haloes from $z = 2$ to $z = 5$, where the time between two simulation outputs varies from

approximately 200 Myr to 100 Myr. This time resolution is good enough to capture merger events reliably and in these time intervals any change in the large-scale distribution of merger remnants is negligible.

Detailed merger trees were constructed for the simulation by identifying haloes and subhaloes with, respectively, a friends-of-friends (FOF) group-finder and an extended version of the SUBFIND algorithm (Springel et al. 2001): particles are included in the same FOF group if their mutual separation is less than 0.2 of the mean particle separation. The SUBFIND algorithm then identifies locally overdense and self-bound particle structures within FOF groups to isolate bound subhaloes (which are required to contain a minimum of 20 particles). For further details on the Millennium Simulation and the tree building procedure we refer the reader to Springel et al. (2005).

The formation and evolution of galaxies has been followed in a post-processing simulation which uses the dark matter merger trees as basic input combined with analytical treatments of the most important baryonic physics in galaxy formation, including the growth of central BHs (Croton et al. 2006; Bower et al. 2006; De Lucia & Blaizot 2007). This has produced remarkably successful galaxy formation models which reproduce a large set of observational findings about the local and high redshift galaxy populations with good accuracy. While not perfect, this match justifies substantial trust in the basic paradigm of hierarchical galaxy formation in CDM cosmologies, and motivates detailed studies of the merger and clustering statistics using the Millennium Simulation. Below we describe our definition of major mergers both for dark matter haloes and galaxies, which lies at the heart of our investigation of the merger bias phenomenon.

2.2   Halo mergers

We note that different definitions of halo formation time have led to somewhat different quantitative conclusions regarding the effect of assembly history on the large-scale clustering of haloes (e.g., Gao et al. 2005; Wechsler et al. 2006; Li et al. 2008). Here we are interested in the possible bias caused by recent merger activity, which might induce a non-trivial relation between the clustering of dark matter haloes and objects whose formation is triggered by mergers (such as quasars). We are therefore not interested in tracking the full mass accretion history of dark matter haloes, but rather want to focus on the violent major merger events that are thought to trigger efficient BH accretion and starburst activity.

In the present work, we consider as *major mergers* those events in which two separate haloes with comparable masses encounter each other for the first time, that is, when they join the same FOF group. At a given time z_n, we define as recently merged haloes those that, at the previous snapshot z_{n-1}, have two or more progenitors belonging to separate FOF groups whose mass (defined through the number of particles of the FOF group) was $> 20\%$ that of the descendant (corresponding to a minimum ratio $m_{\rm sat} : m_{\rm central} = 1 : 4$). This definition of a major merger is similar to the one of Scannapieco & Thacker (2003), who defined as merger remnants haloes that, within the time interval of a single snapshot, accreted at least 20% of their final mass. These authors, however, also considered haloes that experienced considerable smooth mass accretion, whereas we strictly require the merger remnant to be the product of the encounter of two sufficiently massive FOF progenitors. We note that Wetzel et al. (2007) used different definitions of a major merger, finding their results to be independent of the exact definition, as long as a substantial amount of mass is accreted in

a relatively short time. We therefore also expect our results to be robust with respect to the specific value of the mass ratio threshold adopted here.

In our definition of major mergers we also include encounters of groups that at some later time might split again. This can occasionally happen since the FOF algorithm sometimes links two haloes that are just passing close to each other but that in the future will (at least temporarily) separate again. To check whether this might impact our overall results, we also used the merger trees extracted from the Millennium Simulation by Genel et al. (2008), who carefully excluded all mergers of FOF groups containing subhaloes that at a future time will belong to two different FOF groups. Moreover, Genel et al. (2008) define as halo mass the sum of just the gravitationally bound particles. We checked, however, that our results do not change when switching to the Genel et al. (2008) halo trees. The differences from our reference catalogues affect the halo population only at very low redshifts and at low halo masses, much below the ranges of interest here.

We have also checked that our definition of halo mass based on the number of linked particles instead of a spherical overdensity mass estimate does not affect our result. As an alternative to the FOF group masses, we used as group masses the mass within the radius that encloses a mean overdensity of 200 times the critical density, or the mass within the radius where the overdensity is that expected for virialization in the generalized top-hat collapse model for our cosmology. However, we found that this did not lead to any significant differences in the large-scale clustering properties of haloes as a function of mass.

2.3 Galaxy mergers

In the Millennium Simulation, the orbits of dark matter subhaloes are followed until tidal truncation and stripping due to encounters with larger objects cause them to fall below the simulation resolution limit (20 particles, equivalent to a mass of $\sim 1.7 \times 10^{10} \, h^{-1} \, M_\odot$). Galaxies follow the orbits of their host subhalo until this point, and then their remaining survival time as satellite galaxies is estimated using their current orbit and the dynamical friction formula of Binney & Tremaine (1987), calibrated as in De Lucia & Blaizot (2007). At the end of this interval, a satellite galaxy is assumed to merge with the central galaxy of the host dark matter halo, which can either be a subhalo or, more frequently, the main halo of the associated FOF group (Angulo et al. 2008).

In the event of a minor galaxy merger, the cold gas of the satellite galaxy is transferred to the disc component of the central galaxy together with the stars produced in a starburst (as described below); moreover, the bulge of the central galaxy grows by incorporating all the stars of the satellite. If instead a major galaxy merger has occurred, the discs of both progenitors are destroyed and all stars in the merger remnant are gathered into the spheroidal bulge component. In the galaxy formation model studied here, the starbursts induced by galaxy mergers are described using the "collisional starburst" prescription introduced by Somerville et al. (2001): the fraction e_{burst} of cold gas which is converted into stars in the merger remnant is given by: $e_{burst} = \beta_{burst}(m_{sat}/m_{central})^{\alpha_{burst}}$, where $\alpha_{burst} = 0.7$ and $\beta_{burst} = 0.56$, chosen to provide a good fit to the numerical results of Cox et al. (2004).

We define as major merger remnants those galaxies that have, in the immediately preceding simulation output, two progenitors with stellar masses larger than 20% of the stellar component of the descendant (as for the FOF haloes, this imposes a minimum mass ratio $m_{sat} : m_{central} = 1 : 4$). Note that this definition is close, but not identical, to the distinction between minor/major mergers adopted in the underlying galaxy formation model.

3 RESULTS

3.1 Clustering analysis and the excess bias F

We use the standard definition of the *two-point spatial correlation function* as the excess probability for finding a pair of objects at a distance r, each in the volume elements dV_1 and dV_2 (e.g., Peacock 1999):

$$dP = n^2 \left[1 + \xi(r)\right] dV_1 dV_2, \qquad (1)$$

where n is the average number density of the set of objects under consideration.

The *bias* between two classes of objects (e.g., haloes and dark matter) is defined as the square-root of the ratio of the corresponding two-point correlation functions:

$$b_{H,DM}(r) \equiv \sqrt{\frac{\xi_H(r)}{\xi_{DM}(r)}}. \qquad (2)$$

Since the number density of merging objects at a given snapshot is too low for a statistically significant auto-correlation study (see section 4), we adopt a cross-correlation analysis instead. In this case the bias is given by

$$b_{H,DM}(r) \equiv \frac{1}{b_{R,DM}(r)} \frac{\xi_{H,R}(r)}{\xi_{DM}(r)}, \qquad (3)$$

where $b_{R,DM}(r)$ is the bias (relative to the dark matter) of the population we are using as reference in our cross-correlation analysis, and $\xi_{H,R}(r)$ is the cross-correlation function between the haloes and the reference population. By definition, the bias is a function of scale. However, the scale dependence becomes weak or even vanishes at large scales. Since we are here interested in the behavior of the merger bias at very large scales, we estimate the bias on these scales by finding the best constant value over the range $5 < r < 25 \, h^{-1}$ Mpc. This adds robustness to our results by reducing noise from counting statistics.

We can define the merger bias as the excess in the clustering of merger remnants at large scales with respect to the global population of objects selected with similar properties:

$$F(r) = \xi_{M,R}(r)/\xi_{H,R}(r), \qquad (4)$$

where $\xi_{M,R}$ is the cross-correlation between merger remnants and the reference sample, and $\xi_{H,R}$ is the cross-correlation between the global population and the reference sample.

We estimate errors for our measurements using the bootstrap method, generating for each sample 50 bootstrapped samples of the same size, drawn at random from the parent sample and allowing for repetitions (the error estimates converge already when using just a few dozen bootstrap samples). For each bootstrap sample, we calculate the correlation functions, the bias and the excess bias. The standard deviation among these quantities is then taken as error estimate. Recently, Norberg et al. (2008) pointed out that the variance on the two-point correlation function is overestimated when calculated with bootstrap techniques. Keeping this in mind, we deliberately choose the bootstrap method in order to be conservative in our error estimates. Another option would have been to estimate errors by subdividing the whole Millennium volume into subvolumes (for example eight octants) and then to calculate the variance of the $\xi(r)$ measured within individual subvolumes. This
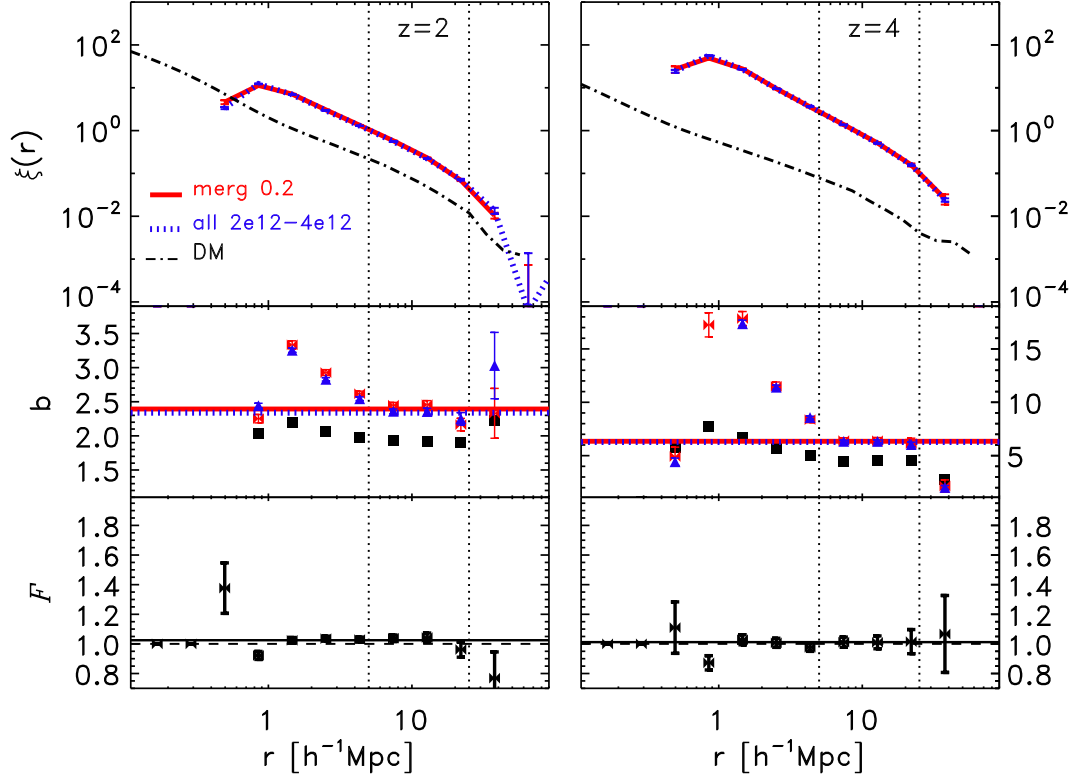
Figure 1. *Upper panels*: Examples of the two-point cross-correlation function at $z = 2$ and $z = 4$ (left and right, respectively) between the reference sample and the haloes with mass in the range $2.0 < M_{\text{Halo}} < 4.0 \times 10^{12} \, h^{-1} \, \text{M}_\odot$ (blue-dotted lines), and between the reference sample and the sub-sample of recently merged haloes (red lines). The auto-correlation of the underlying dark matter is shown as dot-dashed line. *Middle panels*: Bias as a function of scale for all the haloes in the mass bin (blue triangles), for the corresponding merger remnants (red bow-ties) and for the reference sample (black squares). The horizontal lines indicate the fit to the points, over the range indicated by the vertical dotted lines.. *Lower panels*: Excess bias F for the merger remnants relative to the whole galaxy population as a function of scale. The horizontal dashed line indicates $F = 1$. We refer the reader to the text for details of the calculation of errors and the fitting procedure.
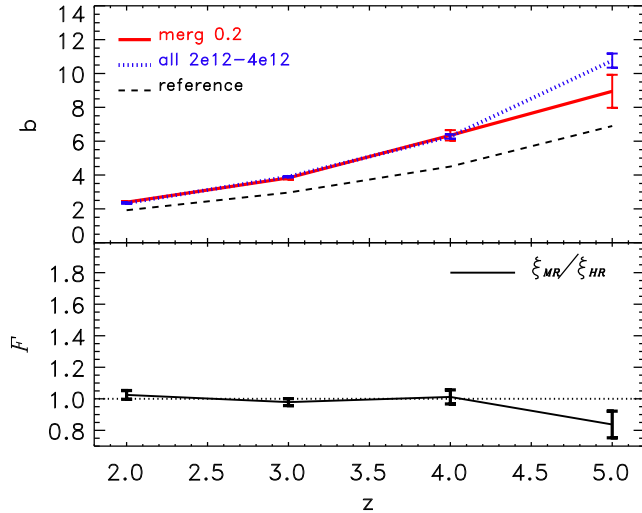

Figure 2. Bias and F parameter as a function of redshift, from the best fit obtained for the halo samples shown in Figure 1.

method becomes inaccurate at large scales (few tens of Mpc) due to the smaller volume probed by each subvolume.

3.2 The merger bias for DM haloes

In our study of the merger bias for haloes we proceed as follows:

• We take all FOF haloes with mass in the range $5 \times 10^{11} < M_{\text{Halo}} < 1.6 \times 10^{13} \, h^{-1} \, \text{M}_\odot$. For the redshifts analyzed in this work, this mass range is well above the collapsing mass M_*, defined by: $\sigma(M_*) = 1.69$ (at $z = 2$, $M_* \sim 1.3 \times 10^{10} \, h^{-1} \text{M}_\odot$). This entire sample is used as reference sample for the cross-correlation analysis. It is large enough that the error on its auto-correlation can be safely neglected with respect to other sources of error in the b and F parameters (it is composed of $\sim 3.5 \times 10^4$ haloes at $z = 5$ up to $\sim 5.5 \times 10^5$ at $z = 2$).

• We subdivide this sample into five mass-bins, with constant logarithmic spacing $\Delta \log M_{\text{Halo}} = 0.3$ (a factor of two in mass). We will refer to these five samples as H_i.

• We then checked which haloes in each of the bins of H_i had a recent major merger, as described in section 2.2. The subsamples of recently-merged objects are denoted by M_i. The fraction of merger remnants is $\sim 10\%$ at $z = 2$, and increases to $15 - 20\%$ at $z = 5$. The mass bins are narrow enough that, within each bin, the merger remnants and the parent population have effectively the same distribution of masses.

For the bootstrap error calculation, we created 50 samples from each of the H_i halo samples, and from these new samples we extracted the corresponding catalogues of the recently-merged haloes.
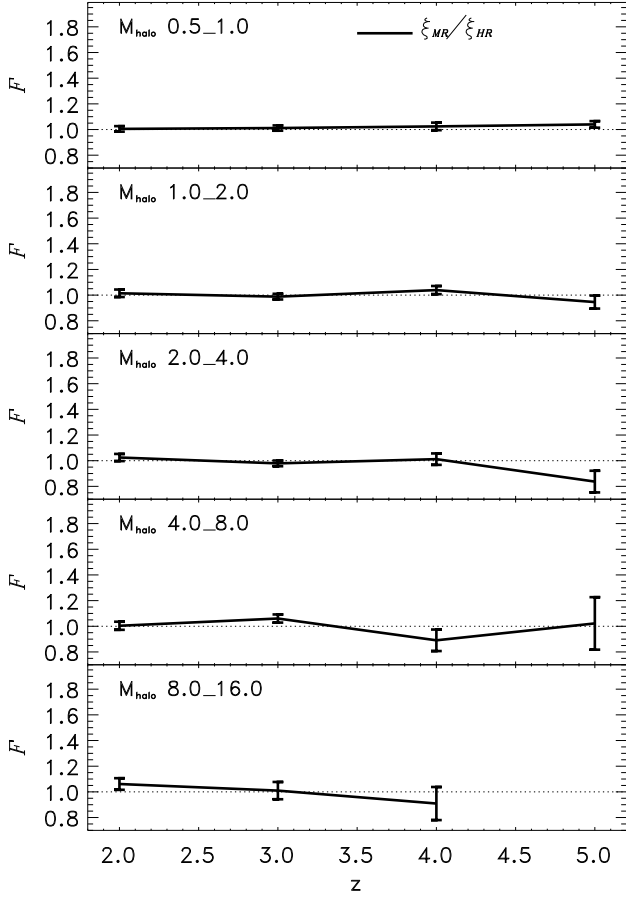
Figure 3. Excess bias for DM haloes in separate mass bins, as indicated in each panel in units of $10^{12} \, h^{-1} \, M_\odot$.

If $\xi_{M_i, R}$ is the cross correlation between the merger remnants and the reference sample, and $\xi_{H_i, R}$ is the cross correlation between all the haloes in the bin and the reference sample, the excess bias parameter is given by $F = \xi_{M_i, R}/\xi_{H_i, R}$. One of our principal aims is to quantify how much F deviates from unity.

In Figure 1, we show at two different redshifts an example of the two-point cross-correlation function, the bias and the F parameter for haloes with masses in the range $2.0 < M_{\rm Halo} < 4.0 \times 10^{12} \, h^{-1} \, M_\odot$. In the top panels, the red and blue curves are the cross-correlation functions between the reference sample and the merger and parent halo samples, respectively. The error bars show the 1σ dispersion of the bootstrap samples. The correlation power drops at small scales as expected for FOF haloes (by definition, two haloes cannot be closer than twice their virial radius, hence the "$1-$halo" term, i.e., the contribution to the correlation function from subhaloes within the virial radius, is missing). In the middle panels, we show at each scale the bias of the merger sample, of the parent sample and of the reference sample (red bow-ties, blue triangles and black squares, respectively); in the lower panels the excess bias $F = \xi_{M_i, R}/\xi_{H_i, R}$ is also shown as a function of scale. The errors on each point on b (and F) are from the 1σ dispersion of the bias (F) calculated for each bootstrap sample. Both for b and F the horizontal lines show the best constant fits to the points in the range $5 < r < 25 \, h^{-1}\,{\rm Mpc}$.

The resulting fits for the bias and F as a function of redshift are shown in Figure 2. The errors on these fits are given by the 1σ dispersion of the fits calculated for each bootstrap sample. The excess bias F corresponding to each halo mass bin considered is shown in Figure 3. If at a given snapshot there are less than 10 mergers, we do not show the result, since the corresponding cross-correlation function would be too noisy. That is why for the higher mass-bins (lower panels) the results are not shown at all redshifts.

In these results, we do not find any statistically significant merger bias, over the full redshift range probed in our analysis. Only in the most massive bins (lower panels), we see a possible signal at the $\lesssim 5\%$ level for the smallest redshift. We stress that switching to the Genel et al. (2008) catalogs or changing our mass definition does not alter the results presented in the Figures discussed above.

3.3 The merger bias for galaxies

We investigated the merger bias of galaxies with a procedure similar to the one adopted above for dark matter haloes. All the galaxies with stellar mass in the range $5 \times 10^9 < M_{\rm star} < 1.6 \times 10^{11} \, h^{-1} M_\odot$ have been divided into five mass bins, G_i, and from each bin we extracted subsamples of recently-merged galaxies M_i, obtained as described in section 2.3. We use as reference sample the entire galaxy population in this range ($5 \times 10^9 < M_{\rm star} < 1.6 \times 10^{11} \, h^{-1} M_\odot$, which is composed of $\sim 10^5$ galaxies at $z = 5$ up to $\sim 1.4 \times 10^6$ at $z = 2$). This sample is again large enough that the error on its auto-correlation can be safely neglected.

In Figure 4, we show an example of the two-point cross-correlation function for the intermediate mass bin. We refer to the description of Figure 1 for details on the derivation of the bias b and the excess bias F. Unlike for FOF groups, where it only makes sense to consider the clustering properties on large scales, for the galaxies we can compute the correlation function down to very small scales $\sim 0.01 \, h^{-1}\,{\rm Mpc}$, allowing for a rather accurate description of the 1-halo term as well, at least at $z < 4$. We find that while F at large scales is approximately constant, it steadily increases at the smallest scales probed by our study. The detection of a steady increase of the excess bias F with decreasing scale might be of potential interest. A comparison between model predictions and the observed small-scale clustering of quasars at different redshift and luminosity thresholds could, in fact, provide insights on the merger-driven nature of quasars, and we postpone a detailed analysis of this subject to future work.

The excess bias F fitted on scales larger than $5 \, h^{-1}\,{\rm Mpc}$ is plotted as a function of stellar mass and redshift in Figure 5 (solid lines). Excess bias of size $20 - 30\%$ ($F \sim 1.2 - 1.3$) is clearly present for all mass bins and at all redshifts, despite the large error bars at the highest redshifts. In essence, we find that, at fixed stellar mass, recently merged galaxies are more strongly clustered on large scales.

We also examined the mass-distribution of the dark matter subhaloes hosting the galaxies considered in this analysis. For galaxies that sit in the main halo of a FOF group, this mass is given by the virial mass of the group (defined as the mass within the radius that encloses a mean overdensity of 200 times the critical density of the simulation), whereas for galaxies that are located in substructures, the parent halo mass is defined simply as the number of particles bound to the substructure (as determined by the SUBFIND algorithm). We found that, for each galaxy bin, the distribution of masses of the host subhaloes is typically log-normal, and peaks at systematically higher subhalo masses for recently-merged galax-
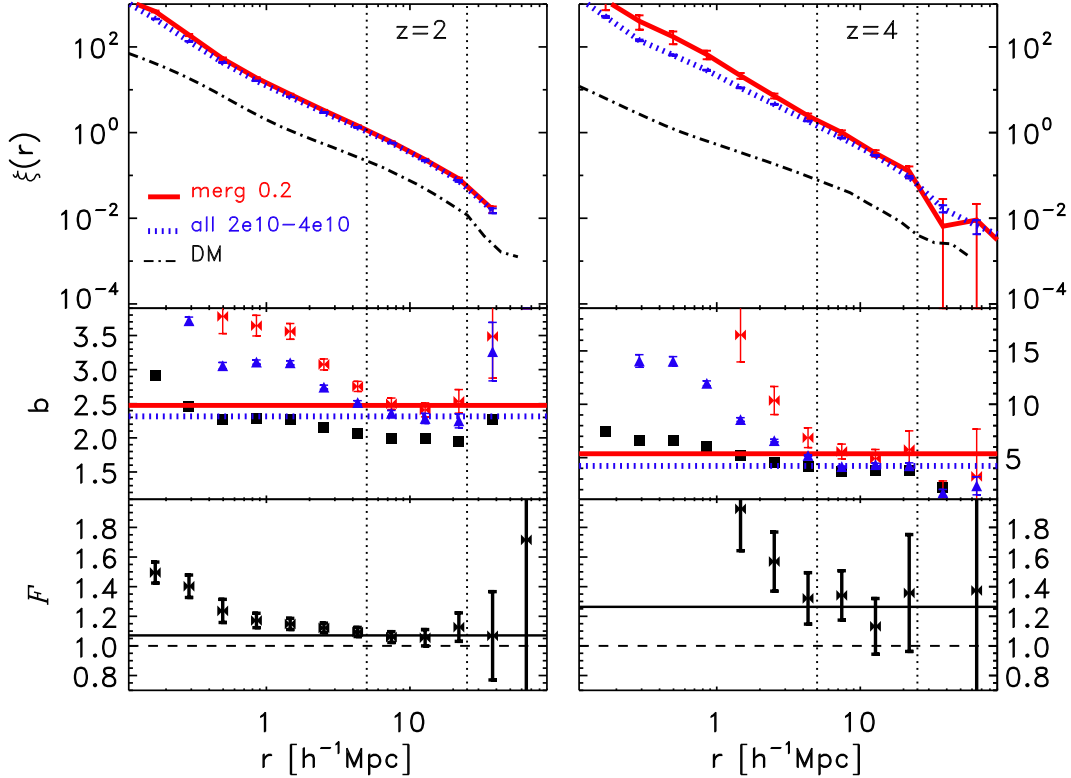
Figure 4. *Upper panels*: Examples of the two-point cross-correlation function at $z = 2$ and $z = 4$ (as labeled) between the reference sample and galaxies with stellar mass in the range $2.0 < M_{star} < 4.0 \times 10^{10} \, h^{-1} M_\odot$ (blue-dotted lines), and between the reference sample and the sub-sample of similar mass merger remnants (red lines). The auto-correlation of the underlying dark matter is shown as dot-dashed line. *Middle panels*: Bias as a function of scale for all the galaxies in the mass bin (blue triangles), for the corresponding merged galaxies (red bow-ties), and for the reference sample (black squares). The horizontal lines show fits to the points, over the range indicated by the vertical dotted lines. *Lower panels*: Excess bias F for the merged galaxies relative to the whole galaxy population as a function of scale. The horizontal dashed line indicates an absence of excess bias (i.e., $F = 1$). We refer the reader to the text for details of the calculation of errors and the fitting procedure.

ies. The median host subhalo masses for the stellar-mass bins are shown as a function of redshift in Figure 6.

This raises the natural question of whether the excess bias detected for galaxies could be due simply to this offset in the typical mass of the host subhalo population. To test this idea, we generated for each galaxy bin a new parent galaxy population with the same distributions of stellar mass *and* host subhalo mass. The excess bias between this "corrected" galaxy population and the corresponding recently-merged galaxies is shown in Figure 5 as a dashed line. This exercise significantly decreases the excess bias signal, and no clear dependence on stellar mass or redshift remains. Nevertheless, a statistically significant excess bias (at the $\sim 10 - 20\%$ level) still seems to be present, especially for the lower stellar-mass bins.

In summary, while for FOF dark matter haloes we did not find any statistically significant merger bias, for galaxies a signal is present at a level of $\sim 10 - 20\%$ for the smallest systems. However, when we restrict ourselves to galaxies at the center of FOF groups ($\sim 75 - 85\%$ of galaxies at $z = 2$ and $\sim 95 - 98\%$ at $z = 5$, depending on stellar mass), the excess bias approaches that obtained for dark matter haloes alone (section 3.2). The differing results obtained for haloes and the galaxy population must therefore be due to the physics of the merger of galaxies, which goes beyond that of halo merging. This is still a topic of active research in galaxy formation modelling.

4   IMPLICATIONS FOR THE CLUSTERING OF QUASARS

The large clustering amplitude of quasars observed by Shen et al. (2007) at high redshift appears to suggest that these objects live in very massive haloes. In Figure 7, the bias associated with FOF halo merger events for different mass ranges and at different redshifts, is compared to the observed quasar bias[1], as calculated by Shen et al. (2009). The high observed clustering is compatible with the clustering associated with the most massive DM haloes, which, at least up to $z \sim 4$, we find to be in better agreement with the analytical predictions of Jing (1998), rather than those of Sheth et al. (2001), though still somewhat higher at the highest redshifts.

As discussed in Section 1, the high observed clustering signal forces quasar models to adopt extreme values for some of the relevant parameters, such as assuming very low scatter in the L-M_{Halo} relation, high duty cycles, and high radiative efficiencies (White et al. 2008; Shankar et al. 2008). However, an excess bias applying specifically to quasar hosts compared with random haloes of the same mass might reduce the need for such strong assump-

---

[1] To correct for the different cosmologies used, the large scale quasar bias measurements from Shen et al. (2009) have been multiplied by $D_{Shen}(z) \, \sigma_{8, \, 0.78}/(D_{Mill}(z) \, \sigma_{8, \, 0.9})$, where D_{Shen} and D_{Mill} are the growth factor calculated for the cosmology used by Shen et al. (2009) and the Millennium cosmology, respectively.
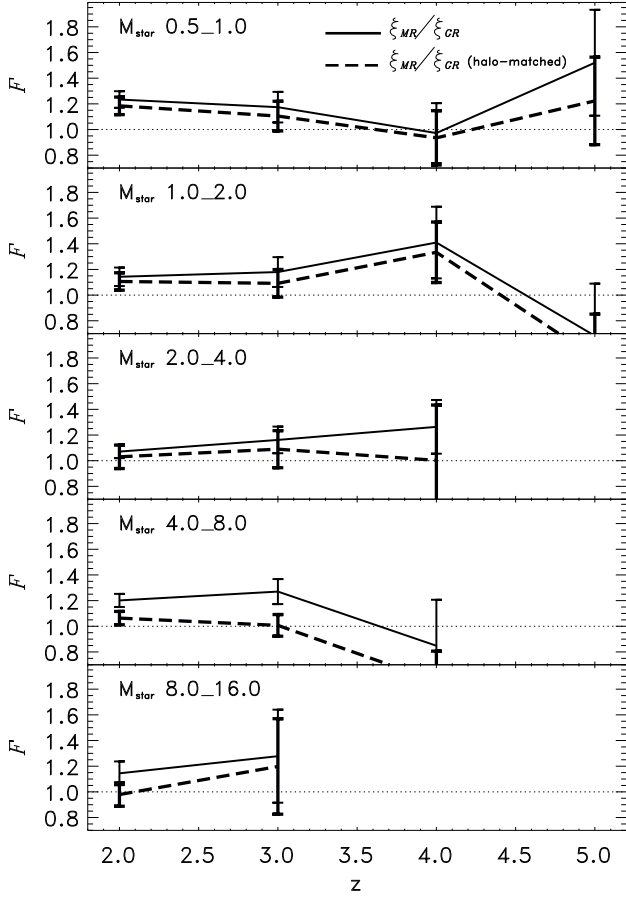
Figure 7. Bias of FOF halo merger remnants as a function of redshift for different mass ranges (as indicated on the plots, in units of $10^{12}h^{-1}M_\odot$). The symbols indicate the bias of bright quasars calculated by Shen et al. (2009), inferred from the clustering observations of Shen et al. (2007).

tions (Wyithe & Loeb 2009). The results of the previous sections for massive haloes and galaxies represent a challenge to this attractive explanation, at least if the excess bias is to be of merger origin. Figure 7 suggests that quasars at $z > 2$ live in haloes $\sim 10^{13}\ h^{-1}M_\odot$ which is broadly consistent with the average host halo mass estimated for lower redshift quasars (e.g., Croom et al. 2005).

If bright quasars have no significant excess bias due to their merger-driven nature, as our results suggest, then either there is another unknown source of excess bias, or, more simply, their clustering must trace the clustering of their host DM haloes and the discrepancy mentioned above must be explained in some other way. At this point it is therefore important to carry out a simple consistency check to see if there are enough massive haloes to host the luminous quasars actually observed in SDSS at $z \gtrsim 3$.

In Figure 8, we compare the number density of observed high-redshift quasars from Shen et al. (2007) with the number density of major halo mergers in the Millennium Simulation. Note that the information extracted from the simulation is a *rate* of mergers, i.e., the number of merger events within the time interval between two snapshots (see Section 2). Therefore, when comparing with quasar number densities we are forced to assume a quasar optical visibility time t_q, that several independent studies have constrained to be relatively short and of the order of $t_q \sim 10^7 - 10^8$ yr (e.g., Shankar et al. 2004; Marconi et al. 2004; Martini 2004; Yu & Lu 2004; Bird et al. 2008, and references therein). In Figure 8 we choose to multiply the rates by a quasar visibility time of 10^8yr, which is, at those redshifts, the approximate time between two snapshots of the Millennium Simulation. The resulting cumulative number densities are plotted in Figure 8 and are compared with the Shen et al. (2007) quasar number densities. The latter, taken from Table 5 in Shen et al. (2007) and converted to our cosmology, are shown with a grey band in Figure 8, which takes into account a factor of two uncertainty due to possible sources not visible in optical surveys due to obscuration.

From this plot we conclude find that if $t_q \gtrsim 10^8$ yr, there are potentially enough mergers of massive haloes in the Millennium Simulation to match the number density and the large-scale clustering properties of $z > 3$ quasars. A merger model would require a fraction 20-25% of haloes with mass $\gtrsim 8 \times 10^{12}\ h^{-1}M_\odot$ to be active at $3 < z < 4$, in nice agreement with the analytical models

Figure 5. Excess bias between merger remnants and the parent galaxy population (solid lines), for different stellar mass bins (the mass range is indicated in the upper-left corner of each panel in units of $10^{10}h^{-1}M_\odot$). The dashed lines show the excess bias after matching the distribution of host subhalo masses. No excess bias is present if $F = 1$ (thin dotted line).
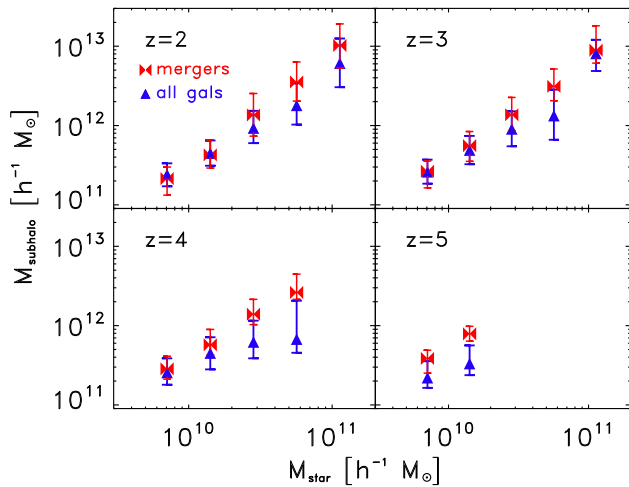

Figure 6. Median host DM subhalo mass corresponding to different stellar masses at different redshifts. The red bow-ties correspond to haloes hosting recently merged galaxies whereas blue triangles refer to the corresponding parent population. The error bars represent the 25 and 75 percentiles of the distribution.
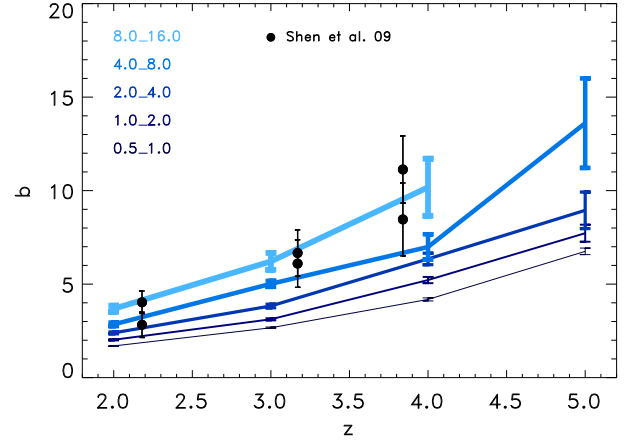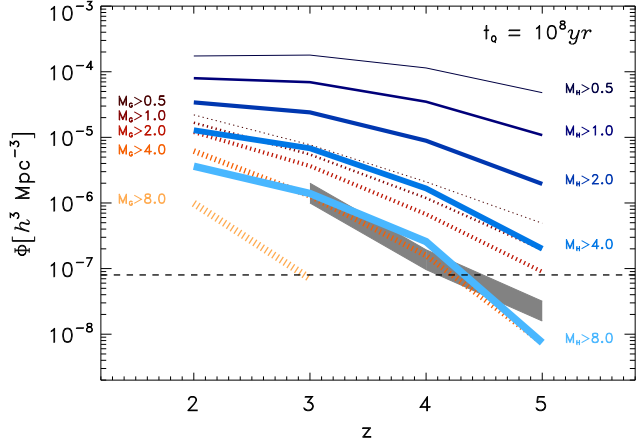
Figure 8. Number density of observed bright quasars from Shen et al. (2007) (gray line), compared with the number of major mergers in the Millennium Simulation, obtained by multiplying the merger rate by a quasar lifetime $t_q = 10^8$ yr. The solid blue lines refer to the cumulative number density of halo mergers, whereas the red dotted lines show the cumulative number of galaxy mergers. The minimum mass corresponding to each line is shown in the plot in units of $[10^{10}h^{-1}\mathrm{M}_\odot]$ for the galaxies and in units of $[10^{12}h^{-1}\mathrm{M}_\odot]$ for the haloes. The number densities quoted by Shen et al. (2007) have been multiplied by a factor of two to account for objects missing from optical surveys due to obscuration.

of Shankar et al. (2008), who find a duty cycle of $0.2 - 0.4$ within the same redshift range. We stress here that our mapping between haloes and quasars neglects any scatter between halo mass and quasar luminosity, which could spoil the agreement as discussed by White et al. (2008). Significant scatter in the $L_{\mathrm{QSO}} - M_{\mathrm{halo}}$ relation would decrease the bias of quasars, since many would be hosted by lower mass (and hence less clustered) haloes.

The red-colored, dotted lines in Figure 8 mark instead the cumulative number densities of galaxy major mergers above different final masses, as labeled. The galaxy model predicts that, on average, the most massive galaxies that recently merged ($M_G \gtrsim 8 \times 10^{10}$ $h^{-1}\mathrm{M}_\odot$) reside in the most massive haloes of mass $\gtrsim 8 \times 10^{12}$ $h^{-1}\mathrm{M}_\odot$, with a stellar-to-halo mass ratio consistent with the one empirically inferred from the cumulative number matching between the stellar and halo mass functions (e.g., Vale & Ostriker 2004; Shankar et al. 2006; Conroy & Wechsler 2008; Moster et al. 2009). However, we find that the number of major mergers for such massive galaxies is below the number of major mergers of the corresponding hosts, as clearly seen in Figure 8 when comparing dotted to solid lines.

This apparent discrepancy is explained, first of all, by the fact that when two haloes merge, their host galaxies will merge at some later time only if the new satellite halo loses enough mass to fall below the resolution limit of the simulation. Moreover, in the current treatment of galaxy mergers, when a galaxy becomes a satellite, it loses its hot gas component; cooling is then inhibited and the stellar component grows only moderately from the cold gas previously available. Therefore, although a given FOF halo merger may be counted as a major merger, by the time the corresponding galaxy merger occurs it may fall below our chosen threshold for a major merger. In any case, despite the fact that the number of major mergers is lower for galaxies than for haloes, the number of mergers of galaxies more massive than ($M_G \gtrsim 4 \times 10^{10}$ $h^{-1}\mathrm{M}_\odot$) is still large enough to explain the observed number densities of bright quasars.

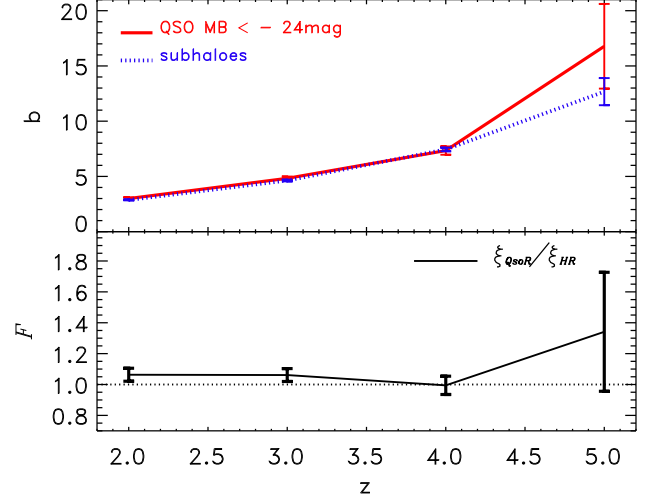**Figure 9.** *Upper panel:* Bias of simulated bright quasars (B-band magnitude < -24 mag), compared with the bias of randomly selected subhaloes with the same mass distribution as the ones hosting the quasars. *Lower panel:* Excess clustering between the two populations.

Taken at face value, the galaxy model would then predict that the SDSS luminous quasars detected at $z > 2$ should be hosted by galaxies as massive as $\gtrsim 4 \times 10^{10}$ $h^{-1}\mathrm{M}_\odot$. Given that virial relations point to BHs more massive than $\gtrsim 3 \times 10^8\mathrm{M}_\odot$, this would suggest an increase, by a factor of $\gtrsim 3$, of the BH-to-stellar mass ratio with respect to local values (Häring & Rix 2004). In addition, we find that the clustering of galaxies with stellar mass $M_G \geqslant 4 \times 10^{10}$ $h^{-1}\mathrm{M}_\odot$ is too weak to match the observed quasar clustering.

To better address the connection with the semianalytical galaxy models, we compare our results with the outputs of the detailed model for the coevolution of quasars and galaxies presented in Marulli et al. (2008) and Bonoli et al. (2009). Figure 9 shows the bias of luminous optical quasars derived using the model of Marulli et al. (2008), built on the assumption that quasar activity is triggered during galaxy mergers. In Bonoli et al. (2009) we showed that such a model predicts well the clustering properties of observed optical quasars at a variety of redshifts and luminosities, independent of the specific light curve characterizing the active phase of a BH. In the upper panel of Figure 9, the bias of bright quasars in the model is compared with the bias of randomly selected dark-matter subhaloes with the same mass distribution as the ones hosting the quasars. The ratio between the two-point correlation functions of the two samples is shown in the lower panel: the excess bias is at most $\sim 5\%$, except at $z = 5$, where the small number of simulated quasars results in a statistically unreliable result.

It is clear that if bright quasars were hosted by DM subhaloes less massive than inferred from the clustering analysis, the BH-to-stellar mass ratio would be even higher (see also the discussion in Shankar et al. (e.g., 2008)). To address, in an independent way, the evolution of the average expected relation between the BH and its host, we compute the expected baryonic mass locked in BHs following the method outlined by previous authors (e.g., Ferrarese 2002; Cirasuolo et al. 2005; Shankar et al. 2006; Shankar & Mathur 2007; Shankar et al. 2008): first, we map haloes to their appropriate virial velocities V_{vir} at a given redshift z applying the virial theorem (e.g., Barkana & Loeb 2001). We then link V_{vir} to the velocity dispersion σ as calibrated in the local universe

by, e.g., Ferrarese (2002), and finally we compute the associated BH mass via the local $M_{\rm BH} - \sigma$ relation (e.g., Tundo et al. 2007). If we assume that these BHs are accreting at an Eddington ratio $\lambda \gtrsim 0.5$, we find that, at $z = 4$, all haloes above $\sim 5 \times 10^{12} h^{-1} {\rm M}_\odot$ can indeed host a BH luminous enough to be recorded in the high-z quasar sample of Shen et al. (2009). This simple exercise proves that if quasars are associated to normally biased haloes, the ratio between BH mass and halo mass could be similar to that observed locally.

5 SUMMARY AND CONCLUSIONS

In the present work we exploited the large halo and galaxy samples extracted from the Millennium Simulation to test the idea that "merger bias", a tendency of recently merged systems to be more strongly clustered on large scales than typical systems of similar mass, could help reconcile the apparent discrepancy between the observed abundance and clustering of high redshift quasars with those predicted for massive dark haloes. Previous studies have, in fact, shown that the quasar number density and clustering can be simultaneously explained theoretically either by models characterized by high duty cycles and negligible scatter in the $L_{\rm QSO} - M_{\rm halo}$ relation (White et al. 2008; Shankar et al. 2008), or by models with non-zero scatter *and* an excess bias for the haloes hosting quasars (Wyithe & Loeb 2009).

We quantify the importance of merger bias at different redshifts and for different halo mass ranges. Defining as major mergers those events in which two friend-of-friend haloes of comparable mass merge into a single system between two simulation outputs, we found that recently merged haloes with masses in the range 5×10^{11} to $1.6 \times 10^{13} \ h^{-1} {\rm M}_\odot$ show no significant excess clustering when compared to other haloes of similar mass.

To connect with physically motivated models of galaxy formation, we also looked for a possible merger bias among samples of galaxies selected from semi-analytical models built on the Millennium Simulation (De Lucia & Blaizot 2007). We considered galaxies with stellar mass in the range $5 \times 10^9 - 1.6 \times 10^{11} h^{-1} {\rm M}_\odot$ and found that merger remnants are typically $10 - 30\%$ more clustered than other galaxies of the same mass. The merger remnants are hosted by systematically more massive subhaloes than other galaxies, explaining a substantial part of this signal. However, even after correcting for this, we still observe excess bias at the level of $\sim 5\%$ for the most massive galaxy merger remnants, and of $\sim 20\%$ for our low-mass objects, which are insufficiently clustered to match the high bias of observed quasars. If we further restrict the analysis to central galaxies (i.e. galaxies at the center of a friend-of-friend group), for which a clear definition of halo mass is available, the excess clustering is once more diminished , approaching the null result obtained for haloes alone.

The clear result obtained for haloes and massive galaxies indicates that merger bias is unlikely to be a viable solution to the apparent puzzle of the high clustering of high redshift quasars. On the other hand, we have also found that recently merged massive haloes with $M_{\rm halo} \sim 10^{13} \ h^{-1} {\rm M}_\odot$ could be both numerous enough and clustered enough to match the observed quasar number density and large-scale bias, if we assume a quasar visibility time $t_q \sim 1 \times 10^8$ yr and if we assume negligible scatter in the relation between halo mass and quasar luminosity.

In conclusion, if major mergers are responsible for triggering quasar activity, the lack of significant merger bias requires models

to be characterized by high duty-cycles and negligible scatter in the relation between quasar luminosity and halo mass.

REFERENCES

Angulo R. E., Baugh C. M., Lacey C. G., 2008, MNRAS, 387, 921

Angulo R. E., Lacey C. G., Baugh C. M., Frenk C. S., 2008, ArXiv e-prints

Barkana R., Loeb A., 2001, PhysRep, 349, 125

Binney J., Tremaine S., 1987, Galactic dynamics. Princeton, NJ, Princeton University Press, 1987, 747 p.

Bird J., Martini P., Kaiser C., 2008, ApJ, 676, 147

Bonoli S., Marulli F., Springel V., White S. D. M., Branchini E., Moscardini L., 2009, MNRAS, p. 606

Bower R. G., Benson A. J., Malbon R., Helly J. C., Frenk C. S., Baugh C. M., Cole S., Lacey C. G., 2006, MNRAS, 370, 645

Cirasuolo M., Shankar F., Granato G. L., De Zotti G., Danese L., 2005, ApJ, 629, 816

Coil A. L., Hennawi J. F., Newman J. A., Cooper M. C., Davis M., 2007, ApJ, 654, 115

Cole S., Kaiser N., 1989, MNRAS, 237, 1127

Conroy C., Wechsler R. H., 2008, ArXiv e-prints

Cox T. J., Primack J., Jonsson P., Somerville R. S., 2004, ApJ, 607, L87

Croom S. M., Boyle B. J., Shanks T., Smith R. J., Miller L., Outram P. J., Loaring N. S., Hoyle F., da Ângela J., 2005, MNRAS, 356, 415

Croom S. M., Smith R. J., Boyle B. J., Shanks T., Miller L., Outram P. J., Loaring N. S., 2004, MNRAS, 349, 1397

Croton D. J., et al., 2006, MNRAS, 365, 11

da Ângela J., Shanks T., Croom S. M., Weilbacher P., Brunner R. J., Couch W. J., Miller L., Myers A. D., et al., 2008, MNRAS, 383, 565

De Lucia G., Blaizot J., 2007, MNRAS, 375, 2

Ferrarese L., 2002, ApJ, 578, 90

Furlanetto S. R., Kamionkowski M., 2006, MNRAS, 366, 529

Gao L., Springel V., White S. D. M., 2005, MNRAS, 363, L66

Gao L., White S. D. M., 2007, MNRAS, 377, L5

Genel S., Genzel R., Bouché N., Naab T., Sternberg A., 2008, ArXiv e-prints

Gottlöber S., Kerscher M., Kravtsov A. V., Faltenbacher A., Klypin A., Müller V., 2002, A&A, 387, 778

Haehnelt M. G., Natarajan P., Rees M. J., 1998, MNRAS, 300, 817

Haiman Z., Hui L., 2001, ApJ, 547, 27

Häring N., Rix H.-W., 2004, ApJ, 604, L89

Hopkins P. F., Lidz A., Hernquist L., Coil A. L., Myers A. D., Cox T. J., Spergel D. N., 2007, ApJ, 662, 110

Jing Y. P., 1998, ApJ, 503, L9+

Kauffmann G., Haehnelt M. G., 2002a, MNRAS, 332, 529

Kauffmann G., Haehnelt M. G., 2002b, MNRAS, 332, 529

Kolatt T. S., Bullock J. S., Somerville R. S., Sigad Y., Jonsson P., Kravtsov A. V., Klypin A. A., Primack J. R., Faber S. M., Dekel A., 1999, ApJ, 523, L109

Lemson G., Kauffmann G., 1999, MNRAS, 302, 111

Li Y., Mo H. J., Gao L., 2008, MNRAS, 389, 1419

Lidz A., Hopkins P. F., Cox T. J., Hernquist L., Robertson B., 2006, ApJ, 641, 41

Marconi A., Risaliti G., Gilli R., Hunt L. K., Maiolino R., Salvati M., 2004, MNRAS, 351, 169

Martini P., 2004, in Ho L. C., ed., Coevolution of Black Holes and Galaxies QSO Lifetimes. p. 169

Martini P., Weinberg D. H., 2001, ApJ, 547, 12

Marulli F., Bonoli S., Branchini E., Moscardini L., Springel V., 2008, MNRAS, 385, 1846

Moster B. P., Somerville R. S., Maulbetsch C., van den Bosch F. C., Maccio' A. V., Naab T., Oser L., 2009, ArXiv e-prints

Myers A. D., Brunner R. J., Nichol R. C., Richards G. T., Schneider D. P., Bahcall N. A., 2007, ApJ, 658, 85

Norberg P., Baugh C. M., Gaztanaga E., Croton D. J., 2008, ArXiv e-prints

Padmanabhan N., White M., Norberg P., Porciani C., 2008, arXiv:0802.2105

Peacock J. A., 1999, Cosmological Physics. Cosmological Physics, by John A. Peacock, pp. 704. ISBN 052141072X. Cambridge, UK: Cambridge University Press, January 1999.

Percival W. J., Scott D., Peacock J. A., Dunlop J. S., 2003, MNRAS, 338, L31

Porciani C., Magliocchetti M., Norberg P., 2004, MNRAS, 355, 1010

Ross N. P., Shen Y., Strauss M. A., Vanden Berk D. E., Connolly A. J., Richards G. T., Schneider D. P., Weinberg D. H., Hall P. B., Bahcall N. A., Brunner R. J., 2009, ArXiv:0903.3230

Scannapieco E., Thacker R. J., 2003, ApJ, 590, L69

Shankar F., Crocce M., Miralda-Escude' J., Fosalba P., Weinberg D. H., 2008, ArXiv:0810.4919

Shankar F., Lapi A., Salucci P., De Zotti G., Danese L., 2006, ApJ, 643, 14

Shankar F., Mathur S., 2007, ApJ, 660, 1051

Shankar F., Salucci P., Granato G. L., De Zotti G., Danese L., 2004, MNRAS, 354, 1020

Shankar F., Weinberg D. H., Miralda-Escudé J., 2009, ApJ, 690, 20

Shen Y., Strauss M. A., Oguri M., Hennawi J. F., Fan X., Richards G. T., Hall P. B., Gunn J. E., et al., 2007, AJ, 133, 2222

Shen Y., Strauss M. A., Ross N. P., Hall P. B., Lin Y.-T., Richards G. T., Schneider D. P., Weinberg D. H., Connolly A. J., Fan X., Hennawi J. F., Shankar F., Vanden Berk D. E., Bahcall N. A., Brunner R. J., 2009, ApJ, 697, 1656

Sheth R. K., Mo H. J., Tormen G., 2001, MNRAS, 323, 1

Somerville R. S., Primack J. R., Faber S. M., 2001, MNRAS, 320, 504

Spergel D. N., et al., 2003, ApJS, 148, 175

Springel V., et al., 2001, MNRAS, 328, 726

Springel V., et al., 2005, Nat, 435, 629

Thacker R. J., Scannapieco E., Couchman H. M. P., Richardson M., 2009, ApJ, 693, 552

Tundo E., Bernardi M., Hyde J. B., Sheth R. K., Pizzella A., 2007, ApJ, 663, 53

Vale A., Ostriker J. P., 2004, MNRAS, 353, 189

Wechsler R. H., Zentner A. R., Bullock J. S., Kravtsov A. V., Allgood B., 2006, ApJ, 652, 71

Wetzel A. R., Cohn J. D., White M., Holz D. E., Warren M. S., 2007, ApJ, 656, 139

White M., Martini P., Cohn J. D., 2008, MNRAS, 390, 1179

Wyithe J. S. B., Loeb A., 2005, ApJ, 634, 910

Wyithe J. S. B., Loeb A., 2009, MNRAS, 395, 1607

York D. G., Adelman J., Anderson Jr. J. E., Anderson S. F., Annis J., Bahcall N. A., Bakken J. A., Barkhouser R., et al., 2000, AJ, 120, 1579

Yu Q., Lu Y., 2004, ApJ, 602, 603